(1̄10) cleaved facet of the waveguide. This means that the incident light is polarised along the ⟨001⟩ crystallographic direction. The electron-to-heavy hole (e–hh) exciton resonance at

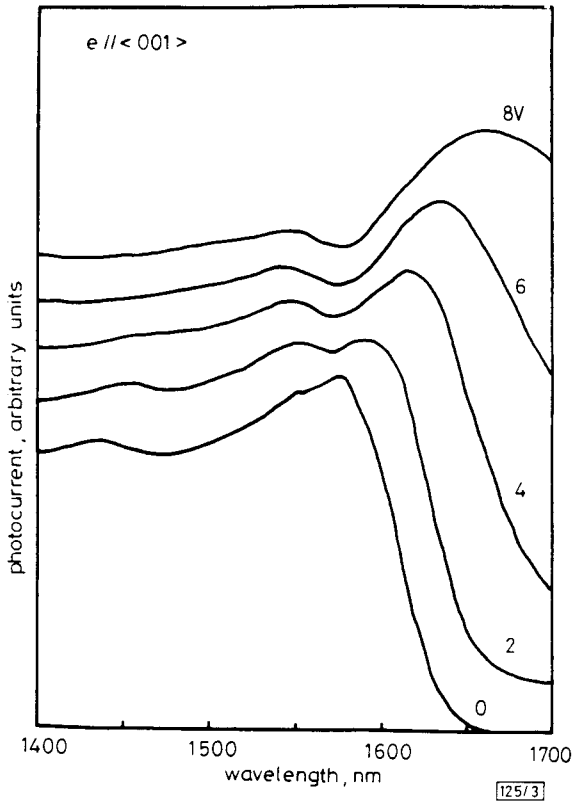

Fig. 3 *Photocurrent spectra as functions of applied reverse voltage*
Spectra are vertically displaced for clarity; photocurrent at 1400 nm is independent of bias voltage; incident light is polarised along ⟨001⟩ crystallographic direction

1·573 μm and the electron-to-light hole (e–lh) resonance at 1·550 μm are clearly observed for zero bias spectra. This shows that the QW structures grown on this unusual substrate by MOVPE are uniform. When the applied reverse voltage is increased, the e–hh absorption peak shifts to a longer wavelength, and the e–lh peak stays near the same wavelength. The photocurrent spectra are vertically displaced for clarity. The photocurrent at short wavelength is independent of bias voltage. This indicates that the intrinsic region is already depleted by built-in voltage and confirms that the impurity concentration in the intrinsic part of the diode is low. The most interesting aspect is that the e–hh exciton absorption is enhanced with the applied voltage. This enhanced exciton absorption with applied voltage has never been reported before. In (100)-oriented QWs, the height of the absorption resonance decreases because of the reduced overlap between the electron and hole wave functions for any material system such as GaAs/AlGaAs, InGaAs/InAlAs, InGaAs/InP, InGaAsP/InGaAsP. In Fig. 3, the height of the e–hh absorption resonance decreases a little when a reverse voltage of 2 V is applied. It recovers and increases concurrently with applied voltages greater than 2 V. Therefore, a new mechanism that enhances the e–hh exciton absorption with the applied voltage seems to be responsible for this peculiar phenomenon. It is presumed that the new mechanism might come from the in-plane anisotropic band structure of the (110)-oriented QW. This result suggests that the field-induced refractive index change associated with this QCSE might be also enhanced and (110)-oriented QWs are very useful in optical modulation and photonic switching applications.

In summary, the quantum-confined Stark effect of an InGaAsP quantum well structure grown on a (110) InP substrate MOVPE has been studied. Clear exciton absorption is observed for the QW. Enhanced exciton absorption concurrent with applied voltage is found when incident light is coupled to the (1̄) cleaved facet. This new QCSE phenomenon might be attributed to the in-plane anisotropic band structure of the (110)-oriented QW. This effect is not only interesting from a scientific point of view but it is also useful in optical modulation and photonic switching applications.

Acknowledgments: K. Oe would like to thank T. Ikegami and T. P. Lee for supporting the collaboration. He also thanks K. Sato for his helpful discussions.

26th May 1992

K. Oe and K. Wakita (*NTT Opto-electronics Laboratories, 3-1, Morinosato Wakamiya, Atsugi, Kanagawa, 243-01, Japan*)

R. Bhat and M. A. Koza (*Bellcore, 331 Newman Springs Rd., Red Bank, NJ 07701-7040, USA*)

References

1 MILLER, D. A. B., WEINER, J. S., and CHEMLA, D. S.: 'Electric-field dependence of linear optical properties in quantum well structures: waveguide electroabsorption and sum rules', *IEEE J. Quantum Electron.*, 1986, **QE-22**, (9), pp. 1816–1830

2 GOOSSEN, K. W., CARIDI, E. A., CHANG, T. Y., STARK, J. B., MILLER, D. A. D., and MORGAN, R. A.: 'Observation of room-temperature blue shift and bistability in a strained InGaAs–GaAs ⟨111⟩ self-electro-optic effect device', *Appl. Phys. Lett.*, 1990, **56**, (8), pp. 715–717

3 GERSHONI, D., BRENER, I., BARAFF, G. A., CHU, S. N. G., PFEIFFER, L. N., and WEST, K.: 'Anisotropic optical properties of (110)-oriented quantum wells', *Phys. Rev. B.*, 1991, **44**, (4), pp. 1930–1933

4 BHAT, R., KOZA, M. A., HWANG, D. M., BRASIL, M. J. S. P., NAHORY, R. E., and OE, K.: 'OMCVD growth of InP, InGaAs, and InGaAsP on (110) InP substrates'. To be presented at Sixth Int. Conf. on Metal-organic Vapor Phase Epitaxy, Cambridge, MA, June, 1992

SELFSTARTING PASSIVELY MODE-LOCKED FIBRE RING SOLITON LASER EXPLOITING NONLINEAR POLARISATION ROTATION

V. J. Matsas, T. P. Newson, D. J. Richardson and D. N. Payne

Indexing terms: Optical fibres, Lasers, Soliton transmission

Nonlinear birefringence effects in a fibre ring laser cavity have been exploited to produce selfstarting, passive modelocking to give 1·5 ps soliton pulses.

Introduction: Selfstarting, passive modelocking of the erbium-doped fibre laser (EDFL) has so far been demonstrated using the nonlinear characteristics of the Sagnac loop mirror [1, 2], or a fast saturable absorber [3]. Nonlinear birefringence [4] has previously been exploited as a selfsustaining mechanism for passive modelocking of fibre lasers [5], but, owing to the short interaction lengths and the relatively highly birefringent fibres used, modelocking could only be initiated by the use of an active modulator. Recent experimental evidence [6, 7], backed by earlier theoretical predictions [8], has demonstrated the feasibility of polarisation switching using lengths of fibre which have a large number of polarisation beats (multibeatlength regime). In a recent paper,* selfstarting, passive, mode locking using nonlinear birefringence was demonstrated using a similar arrangement to that used for this Letter and generating square pulses of a few nanoseconds duration. We report here how the effect can also be exploited for soliton generation.

Experiment: The experimental setup is shown in Fig. 1. The pump source was an argon-ion pumped Ti : sapphire laser providing up to 3 W of CW light at 980 nm to pump the EDFL through a wavelength-division-multiplexing (WDM) coupler which couples most of the pump 980 nm light and almost none of the lasing 1550 nm light. The remaining output

* MATSAS, V. J., NEWSON, T. P., and ZERVAS, M. N.: 'Self-starting passively mode-locked fibre ring laser exploiting non-linear polarisation switching', submitted to *Opt. Commun.*, 1991

port of the WDM coupler served to monitor the launched pump power and for active pump stabilisation using a servo-loop. The cavity comprised 3 m of erbium-doped fibre, 180 m

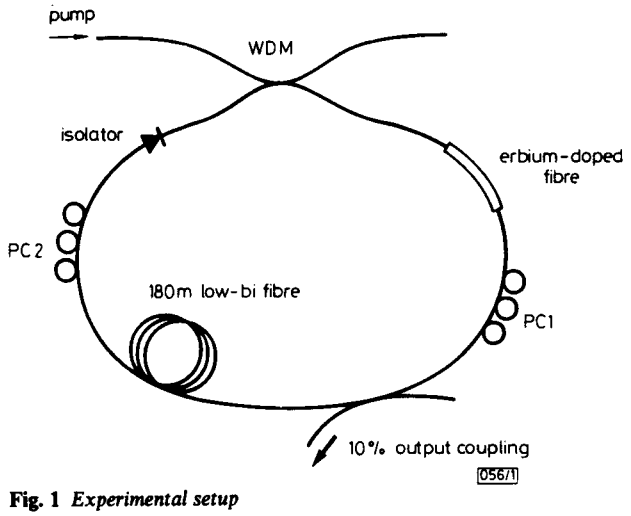

Fig. 1 *Experimental setup*

of passive, low-birefringence spun fibre supplied by York Fibres Ltd., a pigtailed polarisation-dependent optical isolator (OI) (which also serves as a polariser) from BT&D Technology and two sets of polarisation controllers (PCs) placed before and after the low-bi fibre. PC1 controls the polarisation state of the light entering the low-bi section of the cavity and PC2 effectively controls the relative orientation of the polariser (=OI) with respect to the light emerging from the low-bi section. Output coupling was provided by a 90:10 coupler placed immediately after PC1 as shown. The active fibre had an Er^{3+} concentration of 800 *ppm*, $NA = 0{\cdot}15$, and a cutoff wavelength of $\lambda_c = 960$ nm. The passive, low-bi, fibre was characterised by $NA = 0{\cdot}1$, a cutoff wavelength $\lambda_c = 1250$ nm, a group velocity dispersion parameter $D = 17$ ps/nm km at $1{\cdot}56\,\mu$m, an effective core area of $124\,\mu m^2$ and an estimated beat length > 10 m at $1{\cdot}55\,\mu$m.

Because of the presence of a polariser in the ring, the orientation of the PCs controls the total loss of the system. In this way, the output power of the laser could be reduced to as low as 3% of its full power (minimum loss) value, i.e. an extinction ratio of 15 dB. When set in this high-loss condition, the laser is encouraged to operate in pulse mode by the fact that high-intensity pulses cause the onset of nonlinear birefringence and a concomitant swing in the polarisation state reaching the polariser, thereby reducing the resonator loss.

As with the figure-of-eight laser [2], long duration (>500 ps) square pulse behaviour was observed with this system at high pump powers. The square pulses were generated at the cavity round-trip frequency with an optical bandwidth of 30–40 nm. However, at low pump powers (<150 mW) the square pulses became less stable and the system operated entirely in the soliton regime in which the soliton pulses were seemingly randomly spaced within bunches repeating at the cavity round-trip frequency. The laser exhibited a CW threshold of 27 mW launched pump power. With appropriate adjustment of the PCs, selfstarting mode-locking could be initiated by increasing the launched pump power to a 'second' threshold value of 70 mW. Mode locking could then be sustained for launched pump powers down to 27 mW, as shown in the characteristic power hysteresis curve of Fig. 2. Along with an abrupt increase in output power, the onset of mode-locked operation was also marked by an abrupt change in the state of polarisation of the light at the output port, thus proving that the effect is related to the onset of nonlinear birefringence. Discrete power jumps (corresponding to sudden reductions in the number of pulses circulating inside the laser cavity) were observed as the pump power was gradually reduced. This is clearly shown in the inset of Fig. 2. By monitoring the number of pulses in the cavity and recording the change in output power every time a pulse disappeared, we estimated the intracavity pulse energy to be ~48 pJ. An autocorrelation measurement revealed a $sech^2$ pulse shape with a pulse duration of 1·55 ps. The FWHM bandwidth of the optical spectrum (Fig. 3) was 1·68 nm, thus yielding a time-bandwidth product of 0·32. The energy of a fundamental soliton of 1·55 ps duration for the

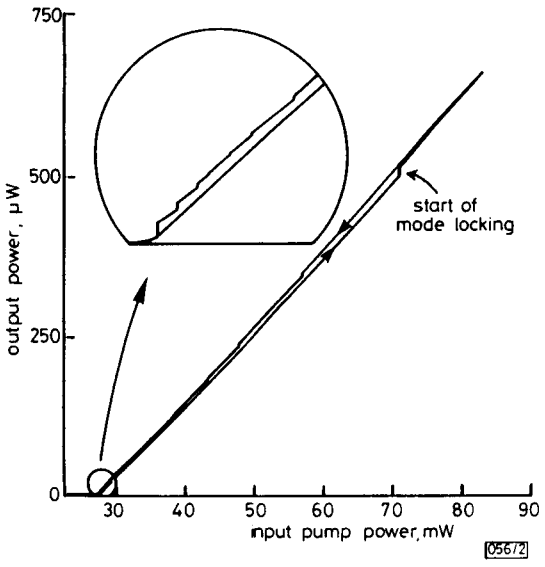

Fig. 2 *Power hysteresis curve*

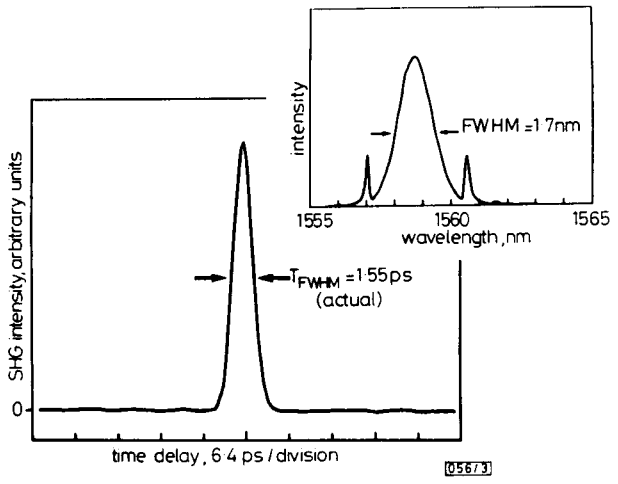

Fig. 3 *Autocorrelation trace and optical spectrum*

parameters given above is 47 pJ, which is in excellent agreement with the measured value of 48 pJ and this indicates that the pulses in the laser are fundamental solitons. Note the two sidelobes located 1·6 nm either side of the main spectral peak in Fig. 3. A log plot indicates that a large number of sidelobes are actually present. As expected, their amplitudes were found to be strongy dependent on the orientation of the PCs (which control the loss of the system) because the sidelobes are a measure of the strength of the various perturbations that a soliton must undergo repetitively as it circulates in the laser cavity [9].

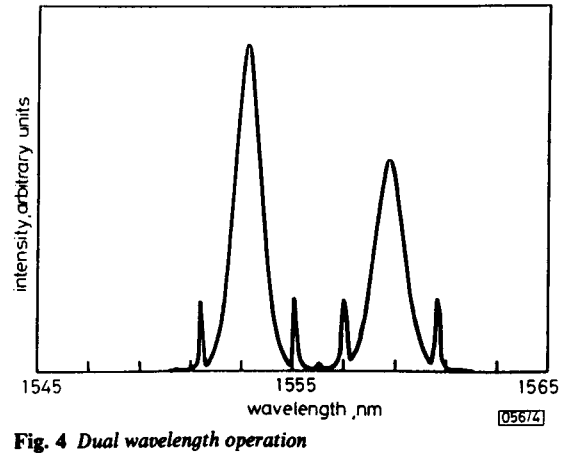

Fig. 4 *Dual wavelength operation*

An important difference between this laser and the figure-eight laser is that in the present case the intensity-dependent loss mechanism that facilitates passive mode-locking varies periodically with wavelength. The difference allows tunable or even dual-wavelength soliton generation, as shown in Fig. 4.

Conclusions: We have demonstrated that nonlinear birefringence can be used in the multibeatlength regime to produce selfstarting, passive mode-locking in an EDFL ring cavity. The pulses obtained have a predominantly $sech^2$ shape and are a few picoseconds long. By stabilising its repetition rate, such a laser could become a tunable source of soliton pulses in the 1·55 μm wavelength region for soliton-based telecommunication systems.

Acknowledgments: V. J. Matsas would like to thank the Committee for Advanced Studies of Southampton University for the provision of a studentship.

19th May 1992

V. J. Matsas, T. P. Newson, D. J. Richardson and D. N. Payne (*Optoelectronics Research Centre, Southampton University, United Kingdom*)

References

1 AVRAMOPOULOS, H. E., HOUH, H., WHITAKER, N. A., JUN., GABRIEL, M. C., and MORSE, T.: 'A passively mode-locked erbium fibre laser'. In Optical Amplifiers and their Applications, Monterey, 1990, PDP8
2 RICHARDSON, D. R., LAMING, R. I., PAYNE, D. N., MATSAS, V. J., and PHILLIPS, M. W.: '320 fs soliton generation with passively mode-locked erbium-fibre laser', *Electron. Lett.*, 1991, **27**, pp. 730–732
3 ZIRNGIBL, M., STULZ, L. W., STONE, J., HUGI, J., DIGIOVANNI, D., and HANSEN, P. B.: '1·2 ps pulses from passively mode-locked laser diode pumped Er-doped fibre ring laser', *Electron. Lett.*, 1991, **27**, pp. 1734–1735
4 AGRAWAL, G.: 'Non-linear fibre optics' (Academic Press, 1990)
5 HOFER, M., FERMANN, M. E., HABERL, F., OBER, M. H., and SCHMIDT, A. J.: 'Mode-locking with cross-phase and self-phase modulation', *Opt. Lett.*, 1991, **16**, pp. 502–504
6 FINLAYSON, N., NAYAR, B. K., and DORAN, N. J.: 'An ultrafast multi-beatlength all-optical fibre switch'. *In*: 'Non-linear guided wave phenomena' (Cambridge, UK, 1991)
7 FERRO, P., HAELTERMAN, M., TRILLO, S., WABNITZ, S., and DAINO, B.: 'Observation of polarisation switching and pulse break-up in spun fibre'. *In*: 'Non-linear guided wave phenomena' (Cambridge, UK, 1991)
8 WINFUL, H.: 'Self-induced polarisation changes in birefringent optical fibres', *Appl. Phys. Lett.*, 1985, **87**, pp. 213–215
9 KELLY, S. M.: 'Characteristic sideband instability of periodically amplified average soliton', *Electron. Lett.*, 1992, **28**, pp. 806–807

FAST WAVELET TRANSFORMS BASED ON THE EXTENDED LAPPED TRANSFORM

H. S. Malvar

Indexing terms: Wavelets, Transforms, Filtering

A new family of wavelet transforms (WTs) based on the extended lapped transform (ELT) is introduced. A new optimisation criterion for the ELT butterfly angles is presented, leading to ELT-based WTs with virtually the same performance but a much lower computational complexity than the standard maximally-regular WTs.

Introduction: Wavelet transforms (WTs) are quite useful for multiresolution signal decomposition [1, 2]. The basis functions of an orthogonal WT correspond to a nonuniform filter bank built as a tree of perfect-reconstruction (PR) two-band filter banks [1–3]. Given a sufficiently smooth lowpass filter as the first WT basis function, all other basis functions will be approximately dilated versions of the same waveform, the wavelet [3, 4].

Smoothness of the lowpass filter (also referred to as the scaling function) is necessary for generating wavelets that correspond to good bandpass filters. This issue can be addressed more precisely using the concept of regularity [3]. In fact, it is possible to guarantee maximum smoothness of the wavelets by using a PR two-band filter bank such that its lowpass filter $H_0(z)$ has a maximum number of zeros at $z = -1$. If the length of $h_0(n)$ is $2N$, there can be at most [3] N zeros of $H_0(z)$ at $z = -1$. When $H_0(z)$ has precisely N zeros at $z = -1$, we call the corresponding WT transform maximally-regular (MR) (note that an MR $H_0(e^{j\omega})$ has a maximally flat response at $\omega = \pi$). For $N \leq 10$, a table of MR filters has been constructed [3].

Although the MR property guarantees maximum smoothness, it is possible to obtain smooth wavelets if $H_0(e^{j\omega})$ is sufficiently small at $\omega = \pi$. In fact, it has been shown [5] that the two-band extended lapped transform [2] (ELT) can be used to generate wavelet transforms with a filtering performance almost as good as that of the MR wavelet transform. The purpose of this Letter is to introduce a new optimisation criterion for the ELT, which leads to ELT-based WTs with the same performance as the maximally-regular WTs.

Extended lapped transforms: The two-band ELT filter bank is defined by [5, 6]

$$h_k(n) = h(n) \cos\left[\left(n + \frac{3}{2}\right)\left(k + \frac{1}{2}\right)\frac{\pi}{2}\right] \tag{1}$$

where $h_0(n)$ and $h_1(n)$ are the impulse responses of the lowpass and highpass filters, respectively, for $n = 0, 1, \ldots, 4K - 1$, where K is referred to as the overlapping factor, and $h(n)$ is a window with even symmetry, $h(n) = h(4K - 1 - n)$, that must satisfy the PR conditions [6]

$$\sum_{m=0}^{2K-2r-1} h(n + 2m)h(n + 2m + 4r) = \delta(r) \tag{2}$$

for $n = 0, 1, \ldots, 2K - 1$ and $r = 0, 1, \ldots, K - 1$.

The ELT filter pair $\{h_0(n), h_1(n)\}$ defined in eqn. 1 can be implemented [2, 5] by the structure in Fig. 1, where the ith orthogonal butterfly is characterised by the transfer matrix

$$\begin{pmatrix} -\cos\theta_i & \sin\theta_i \\ \sin\theta_i & \cos\theta_i \end{pmatrix} = \frac{1}{\cos\theta_i}\begin{pmatrix} -1 & \tan\theta_i \\ \tan\theta_i & 1 \end{pmatrix} \tag{3}$$

where θ_i is the rotation angle.

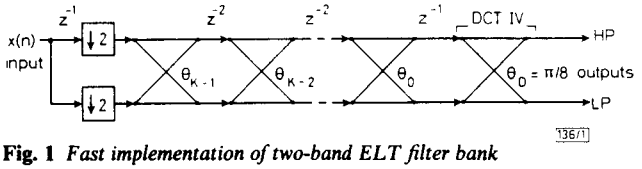

Fig. 1 *Fast implementation of two-band ELT filter bank*

For a given K, there are many windows satisfying eqn. 2. One possible criterion to pick the best $h(n)$ is to minimise its stopband energy, for example [2]. This is based on the fact that the frequency responses of the basis functions are approximately shifted versions of the window response [2]. In the two-band case, however, this approximation is crude, and so we introduce here the idea of minimising the stopband energy of the lowpass filter, because the PR condition guarantees [2, 3] $|H_1(e^{j\omega})| = |H_0(e^{j(\omega+\pi)})|$. Therefore, the butterfly angles of the ELT flowgraph in Fig. 1 can be chosen to minimise

$$E_S = \int_{\omega_s}^{\pi} |H_0(e^{j\omega})|^2 \, d\omega$$

where $\omega_s > \pi/2$ defines the stopband. In Table 1 we have the optimum butterfly angles for $\omega_s = 0{\cdot}725\pi$, obtained by the same nonlinear optimisation procedure [2] that was used to define the ELT angles for more than two bands.